

## Poly (vinylalcohol)-, Polystyrene/Theta Type Zirconium Phosphate Nanocomposite Membranes

S. K. Shakshooki\*

Department of Chemistry, Faculty of Science, Tripoli University, Tripoli, Libya

F. Masaudi

Department of Chemistry, Faculty of Science, Tripoli University, Tripoli, Libya

F. El-Akari

Department of Chemistry, Faculty of Science, Tripoli University, Tripoli, Libya

A. Jangher

Department of Chemistry, Faculty of Science, Tripoli University, Tripoli, Libya

**Abstract:** Novel nanosized theta-type zirconium phosphate,  $\theta$ -Zr(HPO<sub>4</sub>)<sub>2</sub>·1.88H<sub>2</sub>O ( $\theta$ -typeZrP), was prepared and characterized. Its average size particles calculated from XRD broadening method using the Scherer's equation, found to be 60 nm. Transparent flexible thin films of poly(vinylalcohol) (PVA)-, polystyrene(PS) / theta-type zirconium phosphate nanocomposite membranes were obtained from mixing PVA-, PS solutions with different weight percentages of  $\theta$ -typeZrP equal to (5,10,15,20% in wt), respectively. The resultant nanocomposite membranes were characterized by XRD and TGA,. The inorganic filler,  $\theta$ -typeZrP, was well dispersed in the organic polymers matrix, show good thermal and mechanical properties better than that of the original polymers. These nanocomposites are promising for utilizations in fuel cells and as sorbents.

**Keywords:**  $\theta$ -type zirconium phosphate; Polyvinyl(alcohol); Polystyrene nanocomposites.

### 1. Introduction

Layered inorganic ion exchange materials of tetravalent metal phosphates (TVMP) are very insoluble compounds with good thermal stabilities, and possess high ion exchange capacities. They have been known as amorphous for some time [1, 2]. The discovery of their layered crystalline materials [3, 4], represent a fundamental step in chemistry of these compounds. Increase attention directed toward their intercalation [5, 6], catalytic [7], electrical conductance [8], and sensors [9]. Their layered crystalline materials, resemble clay minerals, exist as two dimensional (2-D) and three-dimensional (3-D) structures [10]. Layered two dimensional structure exist in  $\alpha$ ,  $\gamma$  and  $\theta$ -forms of general formula  $\alpha$ -M(IV)(HPO<sub>4</sub>)<sub>2</sub>·H<sub>2</sub>O,  $\gamma$ -M(IV).PO<sub>4</sub>·H<sub>2</sub>PO<sub>4</sub>·2H<sub>2</sub>O,  $\theta$ -M(IV)(HPO<sub>4</sub>)<sub>2</sub>·5H<sub>2</sub>O, respectively [1, 11, 12] (where M = Ti, Zr, Hf, Ge, Sn, Ce ... etc).

Inorganic layered nanomaterials are receiving great attention because of their size, structure, and possible biochemical applications [13], that have been proven to be good carriers for organic polar molecules. Examples of these are zirconium phosphates [14], taking advantage of the expandable interlayer space of the layered materials. Researchers have been capable of encapsulating functional biomolecules into these inorganic matrices protecting them from interacting with environment, avoiding denaturation and enhancing their shelf [13, 15]. Nanoscaled tetravalent metal phosphates and their organic polymer composites comprise an important class of synthetic engineering. However, research in such area is still in its infancy [16-19]. Nanotechnologies are at the center of numerous investigations and huge investments. However, chemistry has anticipated for long the importance decreasing the size in the search of new properties of materials, and of materials structured at the nanosize in a number of applications relate to daily life. Organic-inorganic nanocomposite membranes have gained great attention recently [18, 19]. The composite material may combine the advantage of each material, for instance, flexibility, processability of polymers and the selectivity and thermal stability of the inorganic filler [18-21].

Poly(vinylalcohol)(PVA), hydrophilic and biodegradable polymer, is gaining increase attention, such as proton exchange membranes, and polymer electrolyte fuel cells [22, 23] permeability membranes [24], drug delivery [25]. These applications have stimulate interest in improving the properties of PVA. The interaction between PVA and the nanoadditives [26-28] mainly through hydrogen bonding, which allow efficient load transfer, are responsible for marked increase in mechanical properties. In case of PVA, dispersion and interface interaction are mainly related to the hydroxyl groups in the PVA and the nanoadditives. Polystyrene(PS) is one of the most widely used thermoplastics in many fields, such as electrical appliances, packaging and building materials [18], because of its low cost, rigidity, highly transparencies and chemical stability. Yet, the applications of PS are also limited due to its poor

thermal stability and mechanical property. Limited articles have been reported on the synthesis of  $\alpha$ -zirconium(iv) hydrogen phosphate and fibrous cerium(iv) hydrogen phosphates/polystyrene composites [29, 30]. The layer structured of TVMP can be intercalated with atoms, molecules, small organic groups and even polymers. The structures and properties of the TVMP intercalation compounds can be deliberately tuned, leading to promising potential applications [31]. This paper describes the preparation and characterization of novel nanosized  $\theta$ -type zirconium phosphate and its Poly(vinylalcohol)-, polystyrene nanocomposite membranes.

## 2. Materials and Methods

### 2.1. Chemicals

ZrOCl<sub>2</sub>.8H<sub>2</sub>O, H<sub>3</sub>PO<sub>4</sub> (85%), n-Propyleamine, and Tetrahydrofuran(THF) (of BDH), Poly(vinylalcohol) PVA Mwt = 25125 g/mol, and Polystyrene (of Aldrich), HF(40%) (of Reidle De-Haen). Other reagents used were of analytical grade.

### 2.2. Instruments Used for Characterization

X-ray powder diffractometer Siemens D-500, using Ni-filtered CuK<sub>α</sub>  $\lambda = 1.54025\text{\AA}$ , Xray PANalytical X'PertBRO,Cu Target  $\lambda 1.545\text{\AA}$ . TGA-50 Shumazu Thermogravimetric Analyzer. pH Meter 521 WTW. Fourier Transform IR spectrometer Philips PU 8900.

### 2.3. Preparation of Theta Type Zirconium Phosphate ( $\theta$ -typeZrP)

50ml 0.5M ZrOCl<sub>2</sub>.8H<sub>2</sub>O in 3M HF were mixed with 200ml of (4.6M) H<sub>3</sub>PO<sub>4</sub> in Pyrex round bottom flask (prior to mixing, the solutions were cooled at  $\sim 15^\circ\text{C}$ ). The mixture was left at  $\sim 15^\circ\text{C}$  for 3days. The resultant precipitate was washed with distilled water, by addition and decantation of distilled water up to pH3. The resultant product was filtered and dried in air for 72 hrs at room temperature ( $\sim 25^\circ\text{C}$ ).

### 2.4. Preparation of PVA/ $\theta$ -typeZrP Nanocomposite Membranes

Poly(vinylalcohol) in 10 % concentration was prepared by dissolving 10g of PVA in 125 ml distilled water at  $80^\circ\text{C}$  with stirring for 1h. kept at the same temperature until the total volume is equal to 100 ml.

Different PVA/  $\theta$ -typeZrP nanocomposite membranes were prepared where weight % loading of  $\theta$ -ZrP were (5,10,15,20% inwt). Typically preparation of PVA/ $\theta$ -typeZrP nanocomposite : 0.1g  $\theta$ -typeZrP was dispersed in 5 ml distilled water with vigorous stirring at room temperature for 1 h., to that 9 ml of PVA (10% in concentration) were added with stirring. The stirring was continued at  $45^\circ\text{C}$  for 48 h C. The resultant mixture was poured into flat surface container, of desired thickness, and was allowed to dry in air. The fully dried transparent flexible thin film was peeled from the glass container to obtain PVA/  $\theta$ -typeZrP (10% in wt). Similarly PVA/  $\theta$ -typeZrP (5,15,20% in wt) were prepared using the required mixed ratio.

### 2.5. Preparation of PS/ $\theta$ -typeZrP Nanocomposite Membranes

Polystyrene (PS) in 5% concentration in (THF) was prepared. Different PS/  $\theta$ -typeZrP nanocomposite membranes were prepared where weight % loading of  $\theta$ -typeZrP were (5,10,15,20% in wt). Typically preparation of PS/  $\theta$ -typeZrP(10% in wt) nanocomposite membrane was 0.1g  $\theta$ -typeZrP was dispersed in 5ml THF, with stirring for 1hr, to that 18 ml polystyrene solution (5% in concentration) were added with vigorous stirring at room temperature for 30 min. The stirring was continued at  $45^\circ\text{C}$  for 48 h. The resultant mixture was poured into flat surface container, of desired thickness, and was allowed to dry in air. The fully dried transparent flexible thin film was peeled from the glass container to obtain PS/  $\theta$ -typeZrP (10% in wt). Similarly PS/  $\theta$ -ZrP (5,10,20% in wt) was prepared using the required mixed ratio.

## 3. Results and Discussion

Lamellar  $\theta$ -type, Zr(HPO<sub>4</sub>)<sub>2</sub>.1.88H<sub>2</sub>O( $\theta$ -typeZrP) was prepared and characterized by chemical , XRD, FT-IR and TGA. Its exchange capacity found to be equal 6.5 Meq/g.

### 3.1. XRD of $\theta$ -type Zr(HPO<sub>4</sub>)<sub>2</sub>.1.88H<sub>2</sub>O

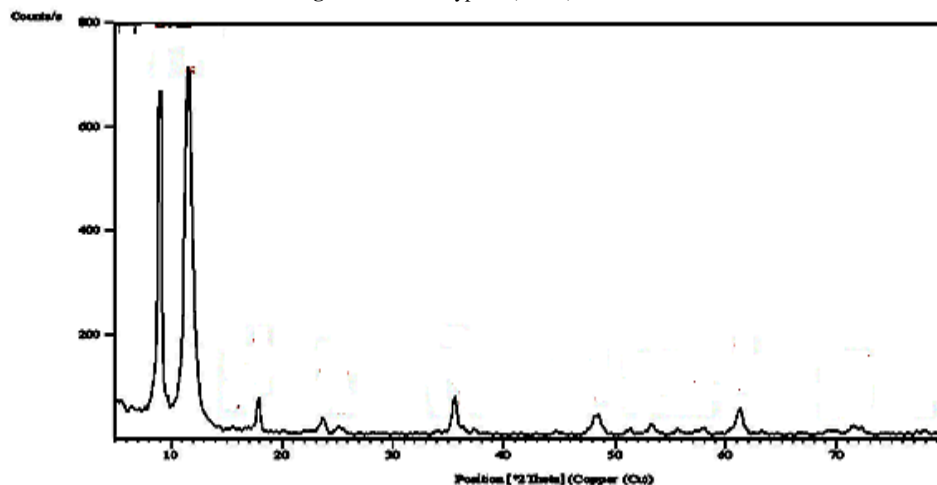
Figure 1 shows the X-ray powder diffraction pattern of the  $\theta$ -type zirconium phosphate, shows the presence of diffraction maxima with two basal spacing equal  $9.85\text{\AA}$  and  $11.65\text{\AA}$ .

Negatively charged layers are formed by macroanions  $[\text{M(IV)(HPO}_4)_2]^{n-}$  and protons ( $\text{H}^+$ ) bonded to the oxygen adjacent to the anionic layer form positively charged layers. The water molecules occupying crystallographic sites are located almost in the center of interlayer cavities. The material exhibit lamellar structure with average size 60nm , that was obtained from using

Scherer's equation;  $D = 0.9 \lambda / B_{2\theta} \text{Cosign } \theta_{\text{max}}$

where  $D$  is the average crystal size in nm (concern apparent particle size),  $\lambda$  is the characteristic wave length of X-ray used ( $\lambda=1.54056 \text{ \AA}$ ),  $\theta$  is the diffraction angle, and the  $B_{2\theta}$  is the angular width in the radius at intensity equal to half of the maximum peak intensity.

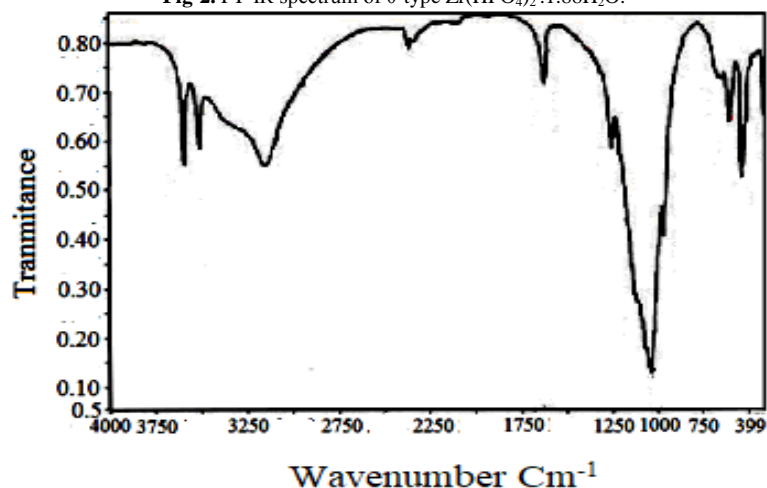
Fig-1. XRD of  $\theta$ -type  $Zr(HPO_4)_2 \cdot 1.88H_2O$ .



### 3.2. FT-IR Spectrum of $\theta$ -type $Zr(HPO_4)_2 \cdot 1.88H_2O$

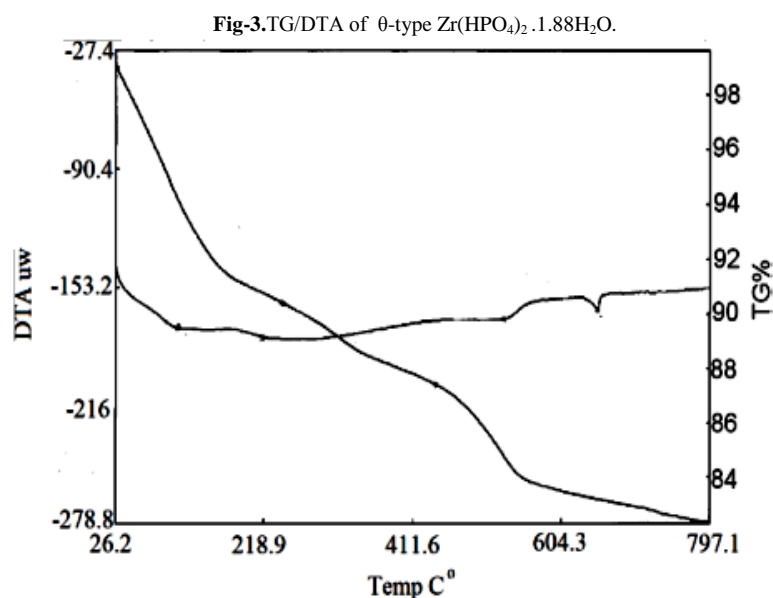
FT-IR becomes a key tool to investigate structure of tetravalent metal phosphate [1, 2, 21]. Figure 2 shows FT-IR spectrum of  $\theta$ -type zirconium phosphate in the range  $4000-400\text{cm}^{-1}$  wave number. The narrow bands at  $3604.65$ ,  $3434.11\text{cm}^{-1}$  and band at  $1640.39\text{cm}^{-1}$  are assigned to vibrational modes of  $H_2O$  molecules, suggest that water molecules are located at well defined crystallographic sites. These bands at  $3434.11$ ,  $3434.11\text{cm}^{-1}$  were also attributed to O-H asymmetric modes of interlayer water molecules. The band at  $1640.39\text{cm}^{-1}$  also corresponds to H-O-H bending modes. The broad band at  $3147.10\text{cm}^{-1}$  assigned to (P)OH stretching mode of the hydrogen bond, it had shoulder at  $3310\text{cm}^{-1}$  attributed to O-H stretching coming from symmetry lowering effect of the  $H_2O$  interlayer molecules. The bands at the region  $1273.21-1054.46 \text{ cm}^{-1}$  are assigned as P-O asymmetry stretching of  $PO_4$  groups, while a band at  $976.33 \text{ cm}^{-1}$  is characteristic to the bonding in plane of the (P-O) bond. The bands in the region  $609.14$  to  $515.39\text{cm}^{-1}$  ascribed to the presence of  $\delta(PO_4)$  and to vibration of water molecules ( $609.14\text{cm}^{-1}$ ), while the band at  $671.64 \text{ cm}^{-1}$  is connected with O-H bond (out of plane). A tentative assignment of various vibration modes is proposed based on previous works performed in other M(IV) phosphate compounds [1, 2].

Fig-2. FT-IR spectrum of  $\theta$ -type  $Zr(HPO_4)_2 \cdot 1.88H_2O$ .



### 3.3. TG/DTA $\theta$ -Type Zirconium Phosphate

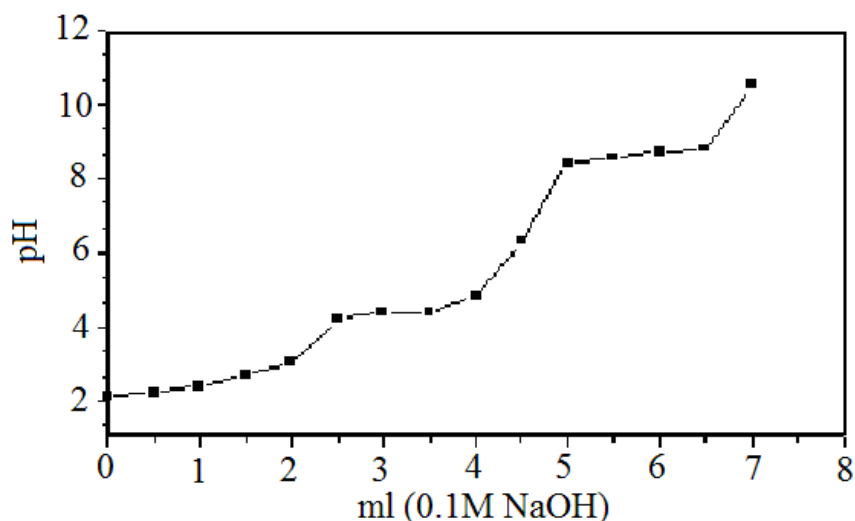
Thermal analysis of  $\theta$ -type  $Zr(HPO_4)_2 \cdot 1.88H_2O$  is shown in Figure 3, was carried out at temperature range  $\sim 25-797^\circ\text{C}$  in air atmosphere. The heating rate was  $10^\circ\text{C}/\text{min}$ . The thermal decomposition exhibits two weight loss stages. The first stage up to  $210^\circ\text{C}$  is accompanied by weight losses equal to  $16.52\%$ , has been attributed to the loss of water of hydration. The second stage in the region  $320-650^\circ\text{C}$  ascribed to the loss of the structure water due to POH groups condensation. The final product was  $ZrP_2O_7$ . The thermal decomposition found to follow the same trends of thermal decomposition of tetravalent metal phosphates [1, 2]. The thermal decomposition was accompanied by four endothermic peaks.



### 3.4. Exchange Capacity of $\theta$ -type Zirconium Phosphate

Exchange capacity of  $\theta$ -type zirconium phosphate was determined by  $\text{Na}^+$  ions titration. The titration curve is shown in Figure 4. The exchange capacity found to be equal to 6.5 Meq/g.

Fig-4.  $\text{Na}^+$  ions titration curve of  $\theta$ -type of  $\text{Zr}(\text{HPO}_4)_2 \cdot 1.88\text{H}_2\text{O}$



### 3.5. Composites of PVA/ $\theta$ -type ZrP

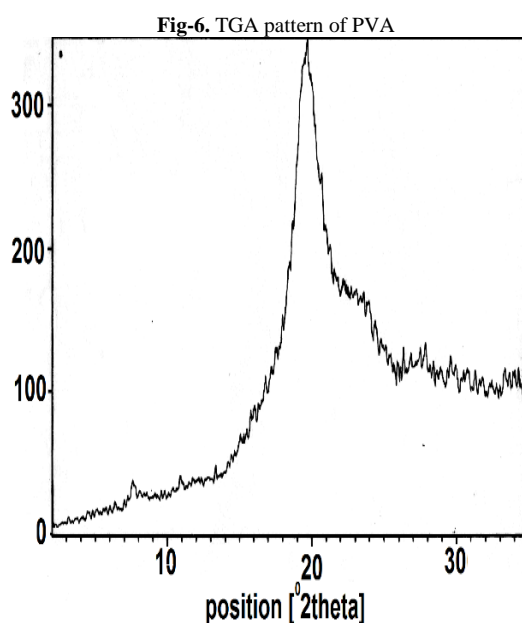
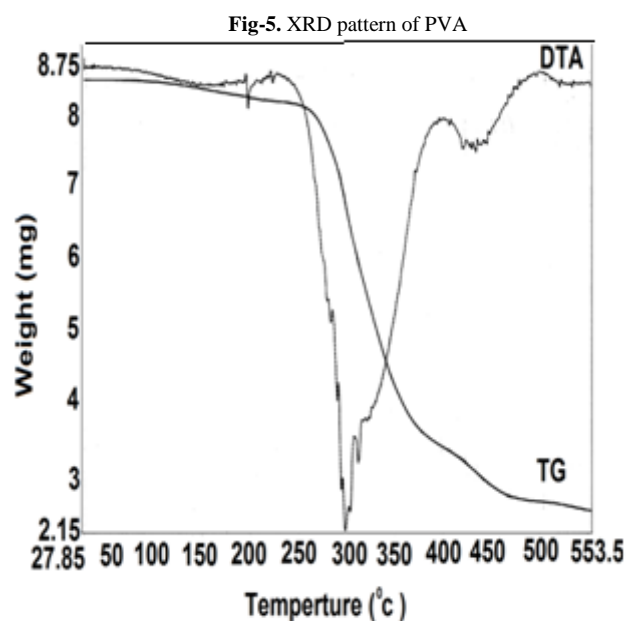
Homogeneous transparent flexible thin films nanocomposites of poly (vinyl alcohol) -, polystyrene /  $\theta$ -type ZrP were prepared and characterized by, XRD, and TGA.

#### 3.5.1. XRD of Poly (vinylalcohol)

Figure 5 shows the XRD of the pure poly(vinylalcohol) with intense peak appearing near  $2\theta = 20^\circ$

#### 3.5.2. TGA of Poly (vinylalcohol)

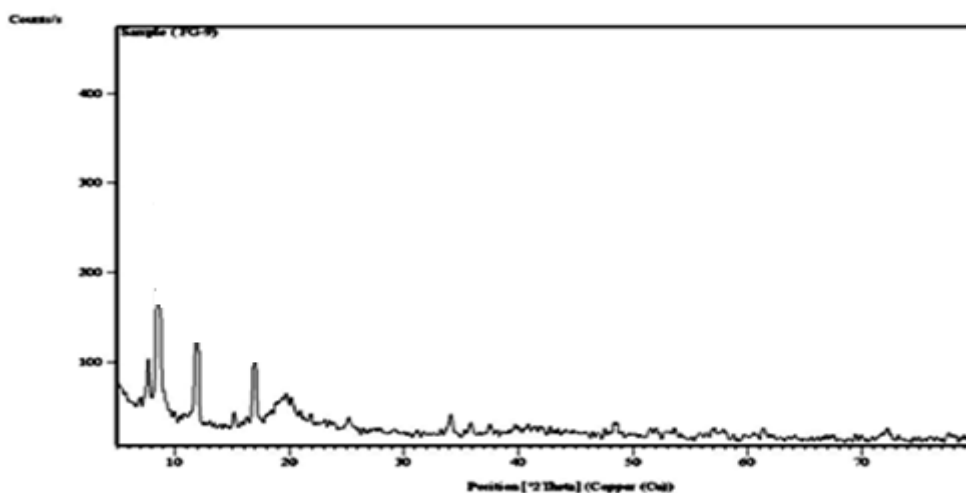
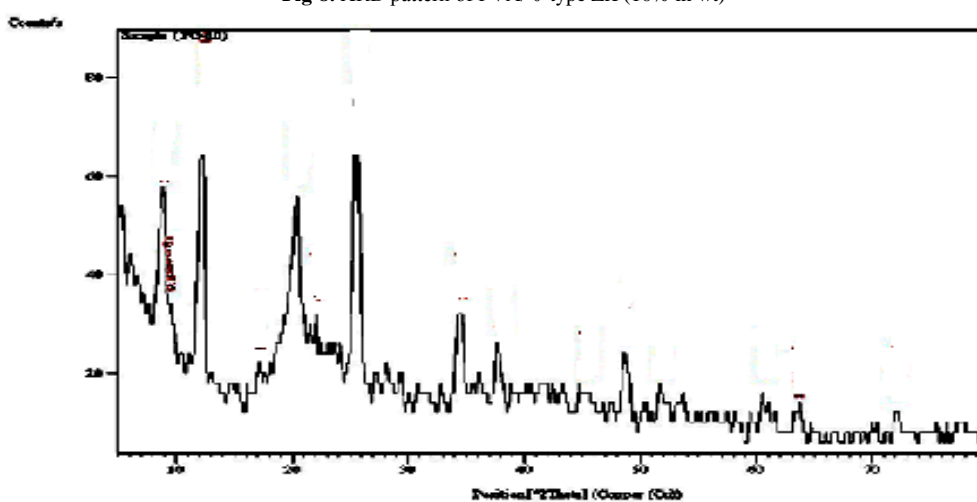
The thermal decomposition of (PVA) is shown in Figure 8. Three temperature regions can be identified over which most of the weight change occurs. The first weight loss occurs between  $75\text{--}115^\circ\text{C}$  corresponds to the loss of water of hydration. The second weight loss occurs  $\sim 300\text{--}360^\circ\text{C}$  corresponds to the side chain decomposition of (PVA). Third degradation between  $410\text{--}600^\circ\text{C}$  corresponds to decomposition of main chain [17] leaving about 42 % residue.



Flexible transparent thin films homogeneous composites of PVA/  $\theta$ -type ZrP were prepared from mixing slurry aqueous solutions of  $\theta$ -type ZrP of different weight percentages (5, 10,15,20% in wt) with aqueous solution of 10% (PVA) in concentration at 45°C and characterized by chemical analysis, X-ray, TGA/DTA.

### 3.5.3. XRD of PVA / $\theta$ -typeZrP

Typical XRD of PVA/  $\theta$ -typeZrP nanocomposites membrane are shown in figures (9,10). Each XRD exhibit peak appearing near 20.1° , which can be assigned to the van der Waal's distance of 4.61Å , characterizing PVA crystalline phase. This peak may be attributed to the strong intermolecular interaction between PVA chains through the intermolecular hydrogen bond. Other peaks are related to  $\theta$ -typeZrP.

Fig-7. XRD pattern of PVA/  $\theta$ -type ZrP (5% in wt)Fig-8. XRD pattern of PVA/  $\theta$ -type ZrP (10% in wt)

### 3. 5. 4. TGA of PVA/ $\theta$ -typeZrP nanocomposite membranes

Figures (9-12) show thermograms of PVA/  $\theta$ -typeZrP nanocomposite membranes of (5,10,15 and 20% in wt loading of  $\theta$ -typeZrP).

Figure 9 shows the TGA of PVA/  $\theta$ -typeZrP (5% inwt). The thermal decomposition occurs in two stages first stage occurs between  $\sim 45$ – $180$   $^{\circ}\text{C}$  corresponds to the loss of water molecules found to be equal to 10.899%. The second stage occurs between  $200$ – $700$   $^{\circ}\text{C}$  correspond to the decomposition of side chain of (PVA), followed degradation of (PVA) main chain and condensation of POH groups of the inorganic materials to pyrophosphate,  $\text{ZrP}_2\text{O}_7$ , leaving 15.23% residue. The thermal decomposition was accompanied with two endothermic peaks at  $150$ ,  $425$   $^{\circ}\text{C}$ .

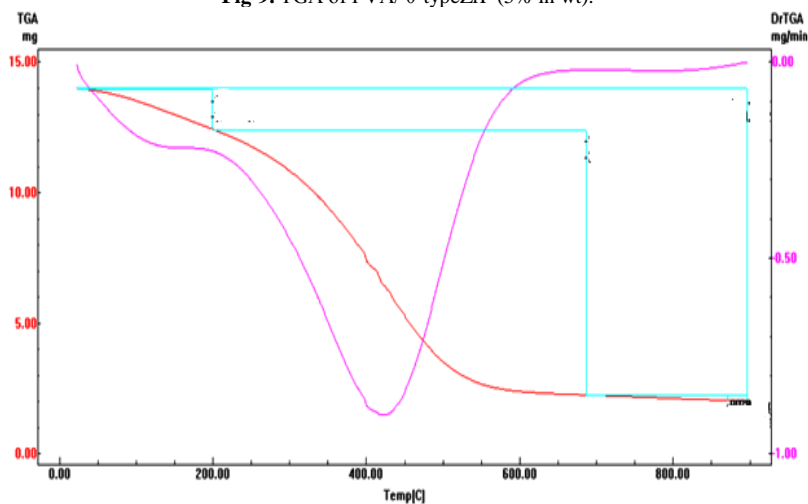
Fig-9. TGA of PVA/  $\theta$ -typeZrP (5% in wt).

Figure 10 shows the TGA of PVA/  $\theta$ -ZrP (10% inwt). The thermal decomposition occurs in three stages first stage occurs between  $\sim 50$ – $175$  °C corresponds to the loss of water molecules found to be equal to 5.179%. The second stage and third stages occur between  $175$ – $900$ °C correspond to the decomposition of side chain of (PVA) , followed degradation of (PVA) main chain and condensation of POH groups of the inorganic materials to pyrophosphate ,  $ZrP_2O_7$ , leaving 15.23% residue. The thermal decomposition was accompanied with three endothermic peaks at 150, 400,750 °C.

Fig-10. TGA of PVA/  $\theta$ -typeZrP (10% in wt)

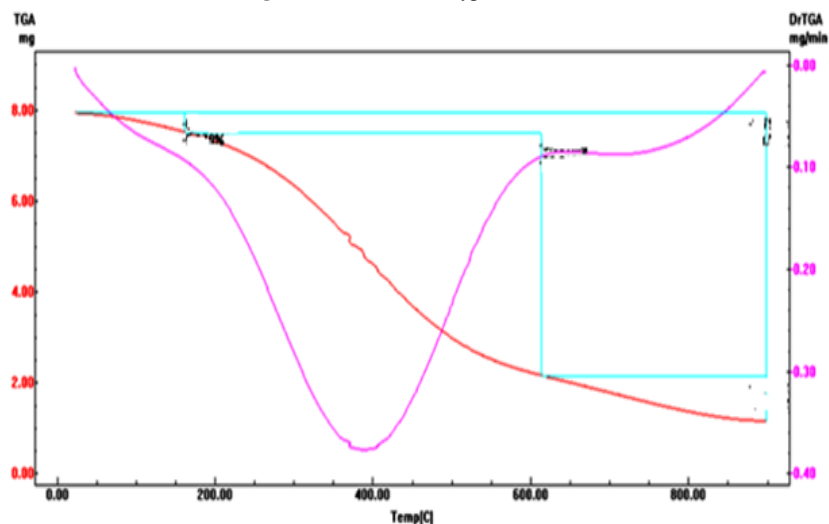


Figure 11 shows the TGA of PVA/  $\theta$ -ZrP (15% inwt). The thermal decomposition occurs in four stages first stage occurs between  $\sim 50$ – $180$  °C corresponds to the loss of water molecules found to be equal to 5.21%. The second stage stages occur between  $180$ – $325$  °C correspond to the decomposition of side chain of (PVA) , the third and four stages occur between  $325$ – $900$  °C corresponds to degradation of (PVA) main chain and condensation of POH groups of the inorganic materials to pyrophosphate ,  $ZrP_2O_7$ , leaving 44.2% residue. The thermal decomposition was accompanied with three endothermic peaks at 150, 275,400, 750 °C.

Fig-11. TGA of PVA/  $\theta$ -ZrP (15% in wt)

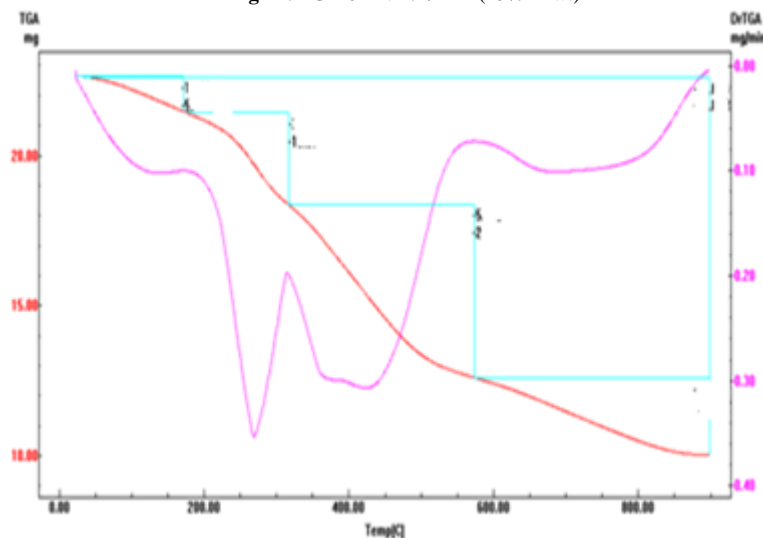
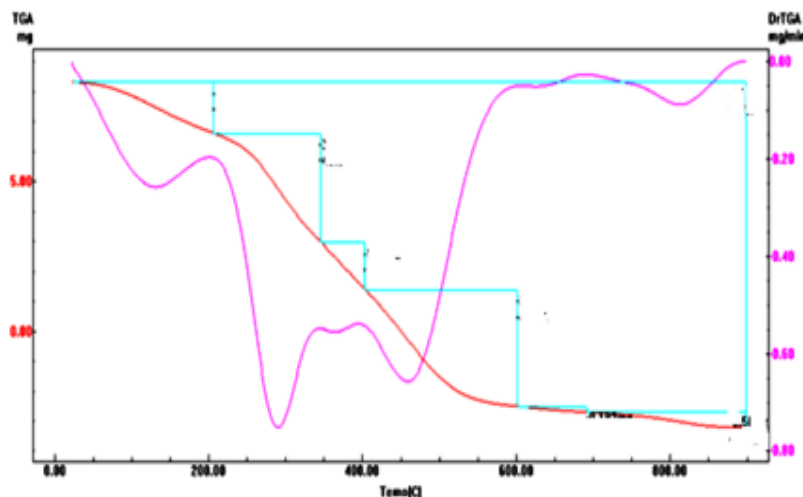


Figure 12 shows the TGA of PVA/  $\theta$ -ZrP (20% inwt). The thermal decomposition occurs in five stages first stage occurs between  $\sim 50$ – $200$  °C corresponds to the loss of water molecules found to be equal to 20.99%. The second stage stages occur between  $200$ – $325$  °C correspond to the decomposition of side chain of (PVA) , the third fourth and fifth stages occur between  $325$ – $900$  °C corresponds to degradation of (PVA) main chain and condensation of POH groups of the inorganic materials to pyrophosphate ,  $ZrP_2O_7$ . The thermal decomposition was accompanied with five endothermic peaks at 150, 285,350, 460, 840 °C.

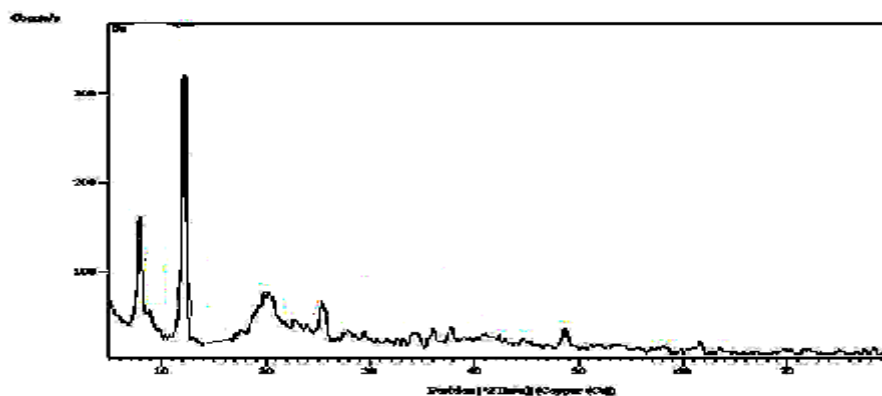
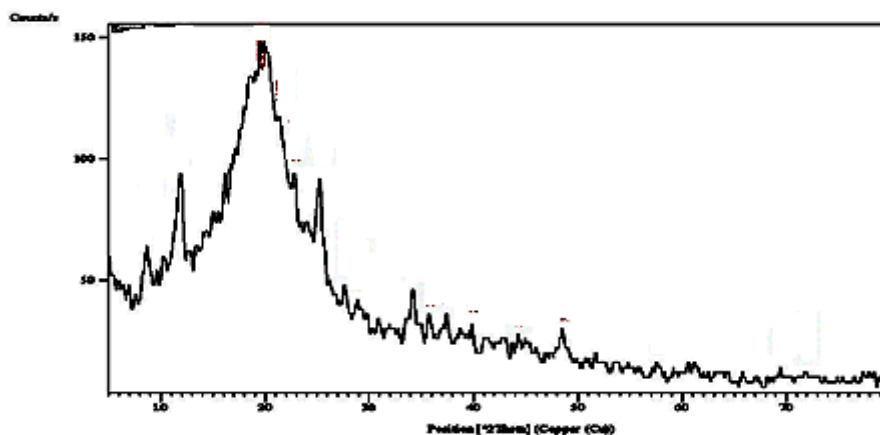
Fig-12. TGA of PVA/  $\theta$ -ZrP (20% in wt).

### 3.6. Composites of PS/ $\theta$ -typeZrP

Homogeneous transparent flexible thin films polystyrene/  $\theta$ -typeZrP nanocomposite membranes was prepared and characterized by, XRD, and TGA.

#### 3.6.1. XRD of PS/ $\theta$ -typeZrP

Typical XRD of PS/  $\theta$ -typeZrP nanocomposite membranes are shown in figures (13,14). Each XRD exhibit peak appearing near  $20.0^\circ$ . Other peaks are related to  $\theta$ -typeZrP.

Fig-13. XRD of PS/  $\theta$ -TypeZrP (5% in wt)Fig-14. XRD pattern of PS/  $\theta$ -typeZrP (10% in wt)

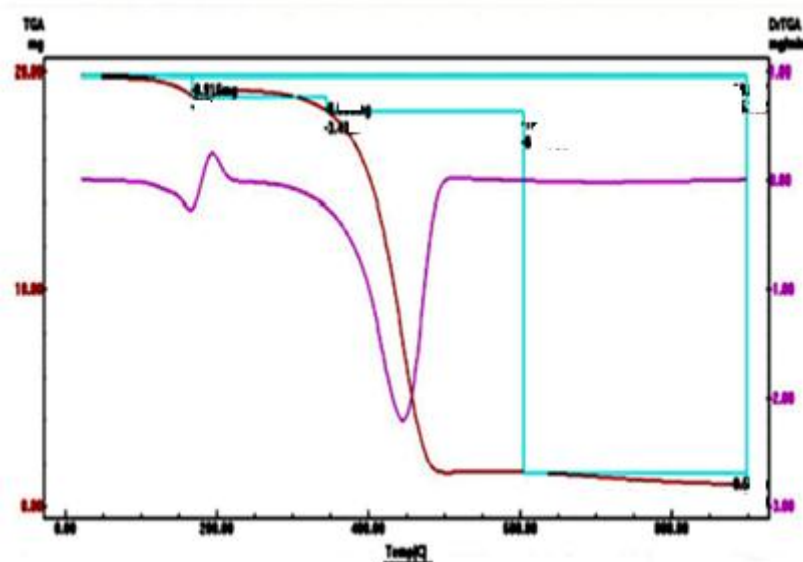
#### 3.6.2. TGA of PS/ $\theta$ -typeZrP

The TGA measurements of PS/  $\theta$ -typeZrP nanocomposites membranes with different mixing ratios of ( $\theta$ -typeZrP = 5,10,15 ,20 % in wt) are shown in Figures (15-18), respectively. The thermal decomposition of the composite materials found to follow almost the same trend, and shows three temperature ranges , can be identified over which most of the weight change occurs.



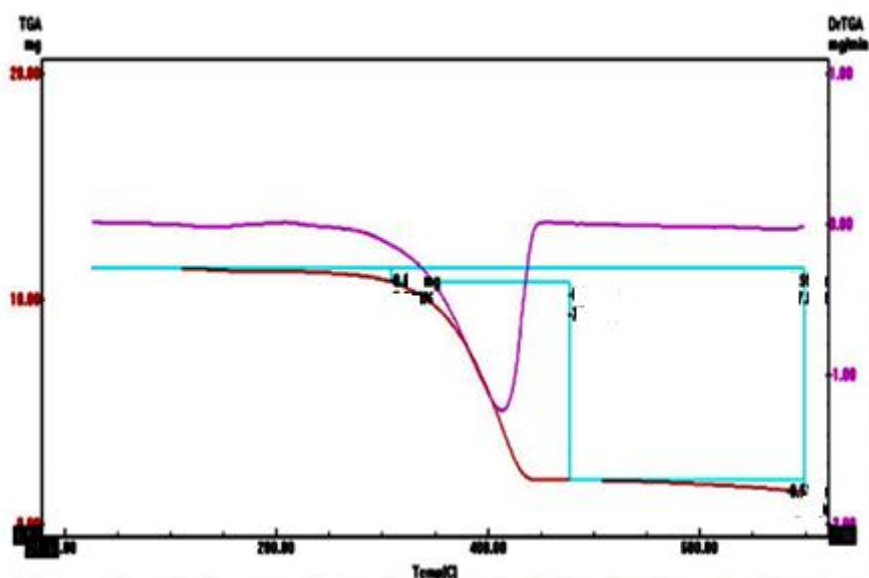
Thermal decomposition of composite membrane of 5% inw ( $\theta$ -typeZrP), is given in Figure 15, shows 4.628% weight loss up to 200°C, which is due to the removal of external water molecules. The weight loss occurs between 200-900°C corresponds to the decomposition of PS and condensation of P-OH groups of the inorganic material to pyrophosphate,  $[\text{ZrP}_2\text{O}_7]$ . The total weight loss found to be 85.18%. Thermal decomposition was accompanied with two endothermic peaks at ~185 and 445 °C. The residue results from thermal decomposition found to be equal to 14.82% .

Fig-15. TGA of PS/  $\theta$ -typeZrP(5% inwt)

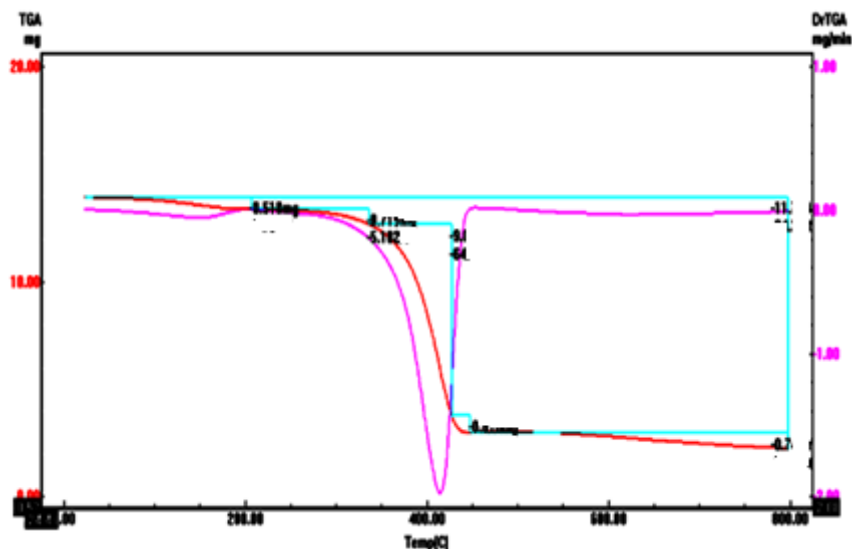


Thermal decomposition of composite membrane of 10% in wt ( $\theta$ -typeZrP), is given in Figure 16, shows no weigh loss up to 230°C , absence of water of external water molecules. The weight loss occurs between 230-800°C corresponds to the decomposition of PS and condensation of P-OH groups of the inorganic material to pyrophosphate,  $[\text{ZrP}_2\text{O}_7]$ . The total weight loss found to be 87.84% . Thermal decomposition was accompanied with two endothermic peaks at ~175 and 420 °C. The residue results from thermal decomposition found to be equal to 12.16%.

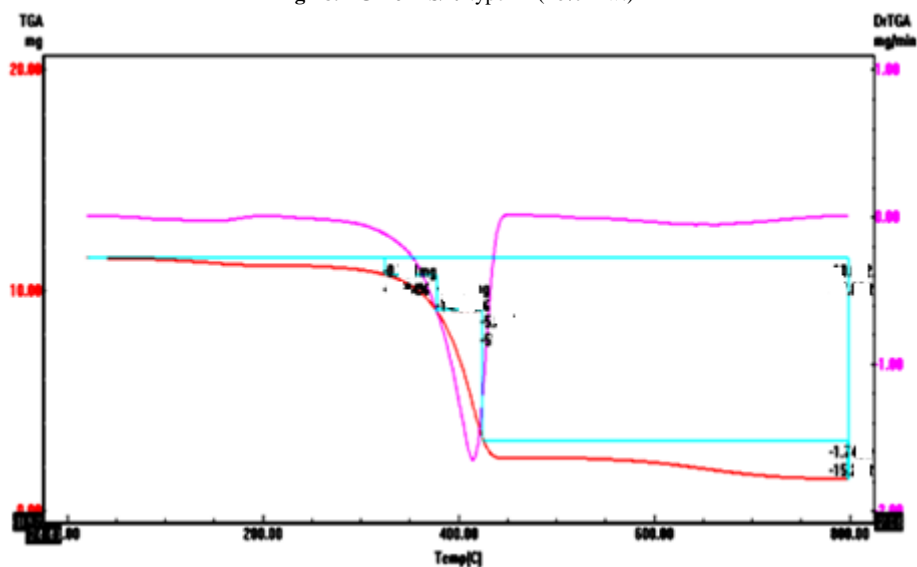
Fig-16. TGA of PS/  $\theta$ -typeZrP(10% inwt)



Thermal decomposition of composite membrane of 15% in wt ( $\theta$ -typeZrP), is given in Figure 17, shows 3.73% weight loss up to 200°C, which is due to the removal of external water molecules. The weight loss occurs between 200-800°C corresponds to the decomposition of PS and condensation of P-OH groups of the inorganic material to pyrophosphate,  $[\text{ZrP}_2\text{O}_7]$ . The total weight loss found to be 84.33% . Thermal decomposition was accompanied with two endothermic peaks at ~175 and 415 °C. The residue results from thermal decomposition found to be equal to 15.67%.

Fig-17. TGA of PS/  $\theta$ -typeZrP(15% inwt)

Thermal decomposition of composite membrane of 20% in wt ( $\theta$ -typeZrP), is given in Figure 18, shows ~3.6% weight loss up to 230°C, which is due to the removal of external water molecules. The weight loss occurs between 230-800°C corresponds to the decomposition of PS and condensation of P-OH groups of the inorganic material to pyrophosphate,  $[\text{ZrP}_2\text{O}_7]$ . The total weight loss found to be 87.82%. Thermal decomposition was accompanied with two endothermic peaks at ~175 and 418 °C. The residue results from thermal decomposition found to be equal to 12.18%.

Fig-18. TGA of PS/  $\theta$ -typeZrP(20% inwt)

#### 4. Conclusion

Nanosized theta type zirconium phosphate,  $\theta\text{-Zr}(\text{HPO}_4)_2 \cdot 1.88\text{H}_2\text{O}$  ( $\theta$ -typeZrP) was prepared., its average size particles found to be 60nm. Series novel nanosized lamellar theta type zirconium phosphate/ poly(vinylalcohol)-, polystyrene nanocomposite membranes were obtained from PVA-, PS solution with different weight percentages of  $\theta$ -typeZrP (5 ,10,15,20% in wt), respectively. The results indicated that PVA-, PS and  $\theta$ -typeZrP posses good miscibility which lead to the formation of homogeneous transparent flexible thin films. The thermal stability was improved. Consequently the presence of  $\theta$ -typeZrP in PVA-, PS favored the increase of the thermal stability and mechanical properties, that may combine physical properties and characteristics of both organic and inorganic components within the single composite. The amount of residues obtained from TGA analysis ranges from ~12-15 % in wt. These composites are promising for utilizations in fuel cells and as new sorbents.

## Acknowledgements

To Department of Chemistry, Faculty of Science, Tripoli University, for providing facilities for this research.

## References

- [1] Shakshooki, S. K., Azzabi, O. H., Khalil, S., Kowalczyk, J., and Naqvi, N., 1988. "Crystalline mixed hafnium-titanium phosphates." *Reactive Polymers*, vol. 7, p. 191.
- [2] Clearfield, A., 1982. *Inorganic ion exchange materials*. CRC Press: Boca Raton, FL. US.
- [3] Clearfield, A. and Styne, J. A., 1964. "The preparation of crystalline zirconium phosphate and some observation on its ion exchange behavior." *J. Inorg. Nucl. Chem.*, vol. 26, p. 117.
- [4] Alberti, G. and Torracca, E., 1968. "Synthesis of crystalline zirconium and titanium phosphate by direct precipitation." *J. Inorg. Nucl. Chem.*, vol. 30, p. 317.
- [5] Costantino, U., 1979. "Intercalation of alkanols and glycols into zirconium(IV) hydrogen phosphate monohydrate." *J. Chem. Soc. Dalton Trans.*, p. 402.
- [6] La-Ginestra, A., Patrono, P., Beradelli, M. L., Golli, P., Ferragina, C., and D., W., 2000. *J. Mol. Cat.*, p. 152-187.
- [7] Vecchio, S., Di-Rocco, R., and Ferragina, C., 2007. "Intercalation compounds of  $\gamma$ -zirconium and  $\gamma$ -titanium phosphates 1,10-phenantroline copper complex materials." *Themochimica acta*, vol. 453, p. 105.
- [8] Thakar, R. and Chudasama, U., 2009. "Synthesis, characterization and proton transport of crystalline zirconium-titanium phosphates." *J. of Sci. and Ind. Res.*, vol. 68, p. 312.
- [9] Alberti, G., Cherubini, F., and Palombari, R., 1996. "Preparation, proton transport and use in gas sensors of thin film zirconium phosphate with  $\gamma$ -layered structure." *Sensors and Actuators*, vol. 2, p. 179.
- [10] Clearfield, A., 1993. "Ion exchange and adsorption in layered phosphates." *Mater. Chem. and Phys.*, vol. 35, p. 257.
- [11] Clearfield, A., Blessing, R. H., and Styne, J. A., 1968. "New crystalline phase of zirconium phosphate." *J. Inorg. Nucl. Chem.*, vol. 30, p. 2249.
- [12] Alberti, G., Bernasconi, M. G., Costantino, U., and Gill, G. S., 1977. "Ion exchange of trivalent cations on zirconium phosphate with large interlayer distance." *J. Chromatog.*, vol. 132, p. 177.
- [13] Colon, J. L., Diaz, A., and Clearfield, A., 2010. "Nanoincapsulation of insulin into zirconium phosphate for oral delivery applications." *Biomacromolecules*, vol. 9, p. 2465.
- [14] Bauer, F. and Porada, M. W., 2006. "Comparison between nafion and a nafion zirconium phosphate nanocomposite in fuel cell applications." *Fuel cells*, vol. 6, p. 261.
- [15] Diaz, A., Saxena, V., Gonzalez, J., David, A., Casanas, B., Carpenter, C., Batteas, J. D., Colon, J., Clearfield, A., et al., 2012. "Zirconium phosphate nano-platelets: a novel platform for drug delivery in cancer therapy." *Chem. Commun*, vol. 48, p. 1754.
- [16] Alberti, G., Casciola, M., Captani, D., Donnadio, A., Narducci, R., Pica, M., and Sganappa, M. N., 2007. "Novel nafion-zirconium phosphate composite membranes with enhanced stability of proton conductivity." *Electrochimica Acta*, vol. 52, p. 8125.
- [17] Yang, Y., Liu, C., and Wen, H., 2009. "Preparation and properties of polyvinyl alcohol / exfoliated zirconium phosphate." *Polymer Testing*, vol. 28, p. 185.
- [18] Nagarale, R. K., Shin, W., and Singh, P. K., 2010. "Progress in ionic organic-inorganic composite membranes for fuel cell application." *Polym. Chem.*, vol. 1, p. 388.
- [19] Shakshooki, S. K., Elejmi, A. A., Khalfulla, A. M., and Elfituri, S. S., 2010. *Int. Conf. on Mater. Imperative*, pp. 49-70.
- [20] Feng, Y., He, W., Zhang, X., Jia, X., and Zhao, H., 2007. "The preparation of nanoparticle zirconium phosphate." *Mater. Letters*, vol. 61, p. 3258.
- [21] Bao, C., Gao, Y., Song, L., Lu, H., Yuan, B., and Hu, Y., 2011. "Facile synthesis of poly(vinyl alcohol)/ $\alpha$ -titanium phosphate nanocomposite with markedly enhanced properties." *Ind. Eng. Chem. Res.*, vol. 50, p. 11109.
- [22] Yang, C. C., Chiu, S. J., and Chien, W. C., 2006. "Development of alkaline direct methanol fuel cells based on crosslinked PVA polymer membranes." *J. Power Sources*, vol. 162, p. 21.
- [23] Helen, M., Viswanathan, B., and Murthy, S. S., 2010. "Poly(vinyl alcohol)-polyacrylamide blends with cesium salts of heteropolyacid as a polymer electrolyte for direct methanol fuel cell applications." *J. Appl. Polym. Sci.*, vol. 116, p. 3437.
- [24] Paralikara, S. A., Simonsen, J., and Lombardi, J., 2008. "Poly(vinyl alcohol) /cellulose nanocrystal barrier membranes." *J. Membr. Sci.*, vol. 320, p. 248.
- [25] Sullad, A. G., Manjeshwar, L. S., and Aminabhavi, T. M., 2010. "Polymeric blend microspheres for controlled release of theophylline." *J. Appl. Polym. Sci.*, vol. 117, p. 1361.
- [26] Salavagione, H. J., Martinez, G., and Gomez, M. A., 2009. "Synthesis of poly(vinylalcohol) /reduced graphite oxide nanocomposites with improved thermal and electrical properties." *J. Mater. Chem.*, vol. 19, p. 5027.
- [27] Cai, D. Y. and Song, M., 2010. "Recent advance in functionalized graphene/polymer nanocomposites." *J. Mater. Chem.*, vol. 20, p. 7906.

- [28] Bao, C. L., Song, L., Guo, Y. Q., and Hu, Y., 2011. "Preparation and characterization of flame-retardant polypropylene / $\alpha$ -titanium phosphate (nano)composites." *Polym. Adv. Technol.*, vol. 22, p. 1156.
- [29] Zang, R. and Hu, Y. O., 2011. "Solvo thermal synthesis of organically modified  $\alpha$ -zirconium phosphate-based polystyrene." *Applied Polymer Science*, vol. 122, pp. 593–598.
- [30] Varsheny, K. G., Tayal, N., Gupta, P., Agrawal, A., and Drabik, M., 2004. "Synthesis, ion-exchange and physical studies on polystyrene cerium(iv) phosphate hybrid fibrous ion exchanger." *Ind. J. of Chem.*, vol. 43, p. 2586.
- [31] Tang, M., Sheng, T., Yue, Y., Mei, Z., Tang, and Zhang, Y., 2016. "A brief review on  $\alpha$ -zirconium phosphate intercalation compounds and nano-composites." *Science China Technological Sciences*, vol. 59, pp. 436-441.